Paper Ref: S2605_P0582
3rd International Conference on Integrity, Reliability and Failure, Porto/Portugal, 20-24 July 2009

GEOMETRIC AND MATERIAL NONLINEAR ANALYSES OF IMPERFECT CIRCULAR HOLLOW SECTION (CHS) COLUMNS: STEEL TUBES AND CONCRETE FILLED TUBES

G. Gonçalves[a], R. C. Barros[a] and M. B. Cesar [b]

[a] FEUP, Faculty of Engineering, of University of Porto, Dept Civil Engineering, Porto, Portugal
[b] Instituto Politécnico de Bragança, Portugal
Email: ge.goncalves@gmail.com , **rcb@fe.up.pt** , brazcesar@ipb.pt

SYNOPSIS

The comparison between theoretical predictions and design curve predictions of the critical stresses, for a wide range of slenderness ratio, is valid and useful. For columns made of steel S235 with initial deformations and slenderness below about 60, columns capacity is controlled by elastic-plastic resistant and performance, as the slenderness decreases (until the minimum limit, controlled by crushing or plastic squash). For columns with slenderness above 60, columns capacity tends to be controlled by elastic instability as slenderness increases. For the used steel S235, in the dimensionless plot of critical stress divided by steel yield stress versus slenderness, the parametric effect of the end-eccentricities is only slightly significant for slenderness between 40 to 80. Rankine-Gordon formula provides conservative safe estimates of the resistant column capacity. The results of the tests of composite columns reveal some of the strength advantage of using composite construction over traditional steel constructions. They also show the importance of top end eccentricities in the results, and the need to ascertain their value with accuracy of about 1-2 mm. Some resistant capacity gains as well as some ductility reductions, are given in tabular form; reasons for possible discrepancy of results are mentioned. The interaction equation for circular section tubes is introduced, and the Merchant-Rankine formula (and its modification) is justified through an example.

INTRODUCTION

Economic and rational developments demand that the structures be functional, economical and with lower construction time. Structures made up of tubular members satisfy such criteria. The columns of concrete filled steel tubes have become common structural elements in modern construction. The increased use is a consequence of its slenderness, high ductility, reduction of assembling time for implementing such structures, and high resistance to fire when adequately coated.

Among the advantages of solely steel tubular columns, one can list: good spatial performance, ductility, excellent performance against the effects of torsion, and speed of the constructive process. For composite columns in steel-concrete, add the following advantages:

- Exemption of the use of formwork, because the tubular profile has both the function of lost formwork in the construction phase, and of reinforcement for the concrete;

- The concrete filling of the column is confined and, therefore, has an higher resistance;

- The use of composite steel-concrete columns permits the use of smaller cross-sections;

- The concrete core increases the column resistance to fire, due to the decrease in reinforcement percentage, and can eliminate or reduce significantly the use of coatings and paint protections;

- The study of high-strength concrete has shown that increasing the elastic capacity of member is not proportional to the concrete resistant capacity to compression.

However, this structural element also has some disadvantages, namely:

- The adherence steel-concrete and the associated normal stresses have been studied in detail, which lead to inappropriate transfer of shear forces. In some special cases it is necessary to use connectors inside the tube;

- The methods of analysis commonly used, only account for normal stress; therefore, the interaction diagrams are not valid;

- The decrease in the size of the sections means an increase in the slenderness, and therefore more columns can become more prone to second-order effects.

The adequate use of structural elements requires knowledge of their behavior to generalized actions imposed upon them during lifetime, including axial loads. In order to reduce some lack of information on column capacities, a comparative study is being done of tubular steel columns and of tubular steel-concrete columns (fundamentally, steel encased concrete columns) to analyze the influence of certain parameters. This article aims to study the behavior of these columns, in the context of stability, for which were then performed two types of analysis: geometrical nonlinear analysis and material nonlinear analysis. Therefore this work consists of an introduction, characterization of materials used, theoretical concepts underlying the analysis, presentation of results and conclusions.

NONLINEAR ANALYSIS OF STRUCTURAL ELEMENTS

The ordinary structural design process is based on the elastic behaviour of the structural elements or the so-called first-order analysis. In this case it is necessary to follow two types of verifications: the resistance capacity to guarantee the structural safety and the serviceability to ensure the proper function during the working life.

Since the real structural behaviour is often complex, the designers usually employ simplified analysis methodologies to verify these two requirements. Basically, these methodologies are based on a simple material structural behaviour; most of the times a linear and elastic behaviour is used, and the assumption that the structural deformation due to the internal efforts is irrelevant and that it does not influence those efforts.

Although this is a normal procedure, there are some structures that require a more detailed analysis to guarantee a truthful result. For these structures the linear first-order analysis must be replaced by a more reliable structural analysis methodology that can simulate the proper material behaviour and the influence of the structural deformation during the loading procedure.

The real material behaviour can be simplified to obtain the desired constitutive law according to the analysis methodology that was selected to study the structural behaviour. In Figure 1 are illustrated several simplified material models that can be obtained from a real constitutive law. In this figure is evident that some material models are simpler than the others. For design purposes elastic and plastic analyses are often chosen because they are based on simple stress-strain relationship. In plastic analysis and design the collapse load becomes the design criterion and this load is found from the material strength (steel in this case) in the plastic range. This is a fast methodology that can provide a remarkable economy since the sections required by this method are smaller than those required by an elastic analysis.

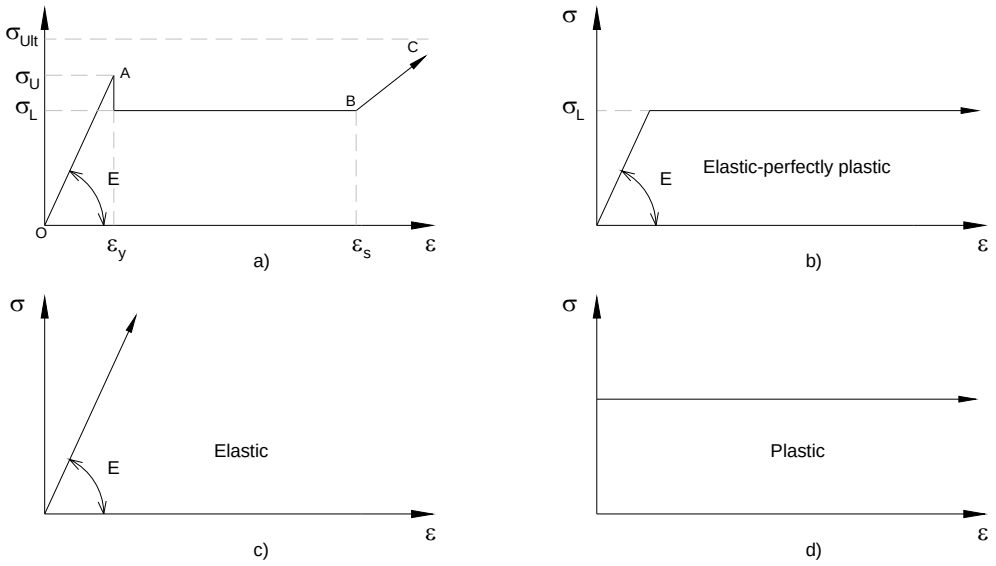

Figure 1: Simplified stress-strain constitutive laws

Although material nonlinearity is one of the most important sources of nonlinear structural behaviour, it is important to realize that this nonlinearity is often associated with a nonlinear geometric behaviour, namely in slender structures because those can have a significant nonlinear response before reaching the resistant capacity as shown in Figure 2.

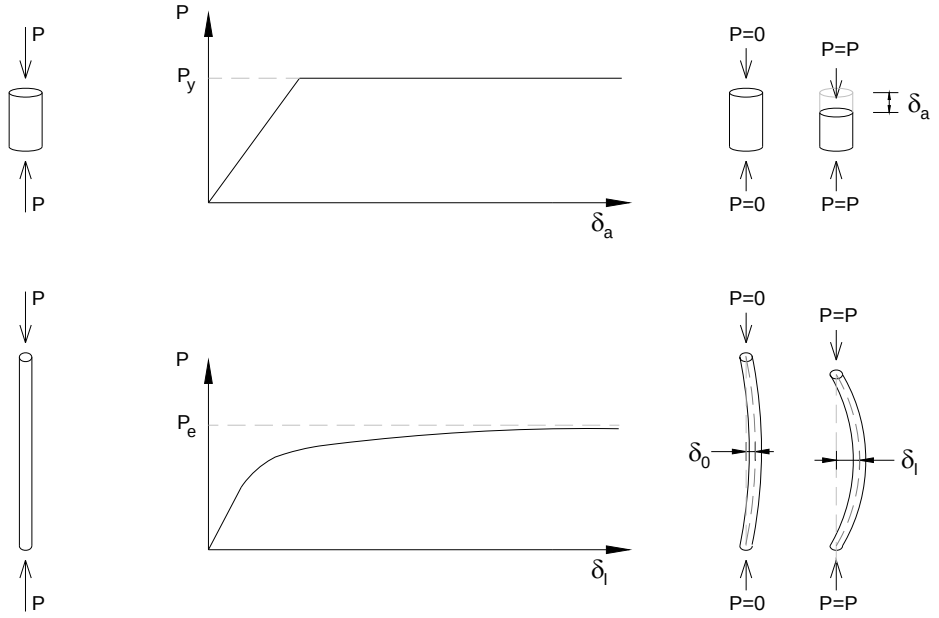

Figure 2: Nonlinear behaviour of a column.

If an elastic behaviour is expected when a large loading is applied, then it is possible to exclude the material nonlinearity and in this case only a nonlinear geometric analysis can be done. In this case, the source of the nonlinearity is related with initial imperfections in the structural members, global deformation of the structure (P-Δ effect) or local deformation of the structural members (P-δ effect), as shown in Figure 3.

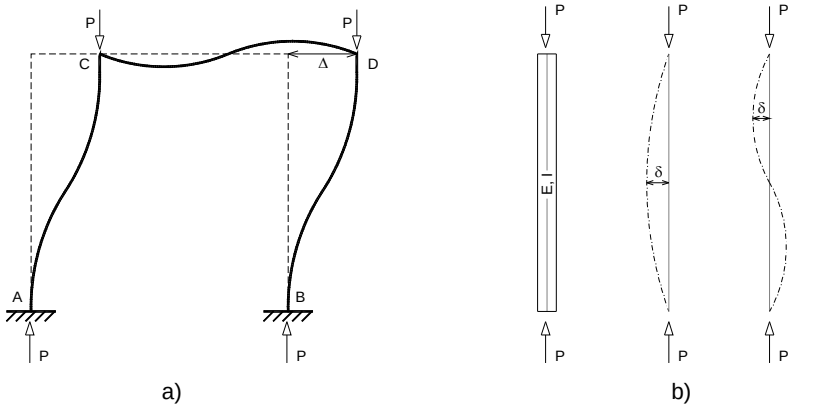

Figure 3: The two P-Delta effects: (a) P-Δ ; (b) P-δ .

In real life, the structural behaviour is always nonlinear and the simplified analysis is only valid for small stress levels and for specific configurations where the linear equilibrium is possible. However, there are structures in which it is impossible to apply these simplifications and their analysis can only be performed with a nonlinear methodology such as the structure shown in Figure 4.

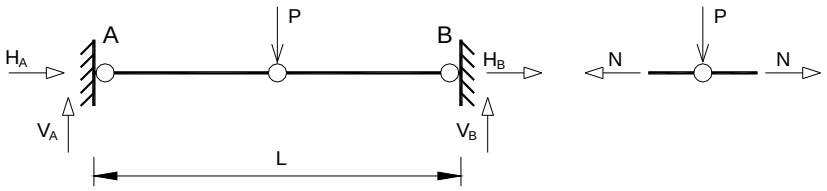

Figure 4: Structural scheme and undeformed equilibrium.

In this case is easy to verify that a first-order analysis (analysis performed with an undeformed structural configuration) does not allow computing the axial effort in the structural members since the equilibrium is not possible at the centre node. The solution to these types of structural systems is obtained by performing a large-displacement analysis, i.e. a nonlinear geometric analysis, where the equilibrium is achieved in the deformed structural configuration as shown in Figure 5.

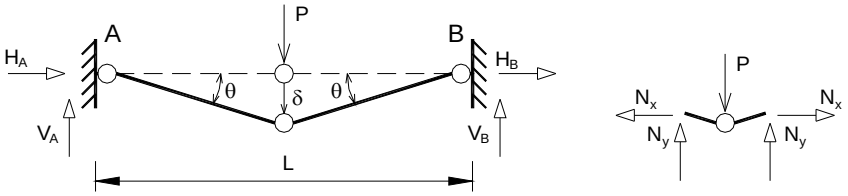

Figure 5: Equilibrium in the deformed structural configuration.

Thus, a geometric nonlinear analysis is carried out when a structure undergoes large displacements and the change of its geometric shape causes a nonlinear displacement-strain relationship. In this case, the structure exhibits significant change of its shape under applied loads such that the resulting large displacements change the coordinates of the structure or additional loads induced. So, the equilibrium relationships are written with respect to the deformed structural shape and the analysis is referred as a second-order analysis. Unlike the first-order analysis, a second-order analysis requires an iterative procedure to obtain solutions since the deformed shape is not known during the equilibrium formulation.

Obviously, there are many possible structural simplifications that can be obtained from the real structural behavior and Figure 6 shows a schematic representation of the possible refined and simplified models that can be used to perform a structural analysis.

In this context, in this article is intended to perform geometric and material nonlinear analysis of slender steel Circular Hollow Sections (CHS) subjected to an increasing axial load. Two phases are involved in this study: the first one is related with the compression of a simple supported CHS steel column and the second phase involves the same type of analysis but with the CHS steel column filled with concrete.

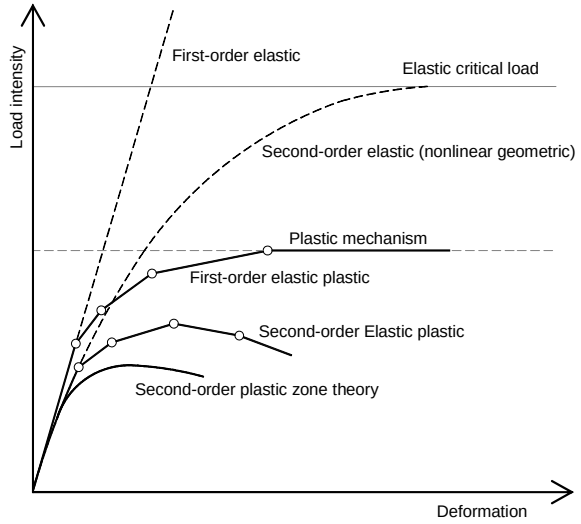

Figure 6: Load-deflection behaviour of plane frames.

THEORETICAL AND DESIGN CURVES OF IMPERFECT CHS STEEL COLUMNS

In this paragraph some analytical results are presented on the analysis of imperfect circular tubular steel columns, particularly with initial deformations and load eccentricities.

The columns studied are of the steel standard S235, have a diameter of 50 cm and a thickness of 1 cm, and have variable length and thus variable slenderness ratio. Regarding the latter, the slenderness ratio is bound by the slenderness limit beyond which the columns buckle elastically. The initial deformation pattern was established for a maximum deformation at mid-height as provided by Eurocode 3 – EC3 (2005).

For columns with imperfections of load eccentricities, three cases of eccentricity amplitudes are analyzed: *i/10*, *i/20* and *i/40* (where *i* is the radius of gyration of column cross section).

The curves of critical ultimate stresses for small and intermediate slenderness range, obtained from this analysis for the 2 types of imperfections, were compared in dimensionless plots with some theoretical and design curves, namely: Euler-hyperbole (Euler), Rankine-Gordon curve (RG) and multiple curves of resistance (as curve "*a*", presented in the above legislation EC3).

These curves are shown in Figure 1 (for columns with imperfection of initial deflections) and Figure 2 (for columns with imperfection of load eccentricities).

In both figures there is an additional curve (different from the theoretical curves listed above) corresponding to the ultimate stresses evaluated from the ultimate load that was determined with the software TBCOL according to the nonlinear methodology detailed in Barros (1983) for spatial tubular beam-columns.

From Figure 7, the curve resulting from the analysis of columns with initial deflections is below the Euler curve, above the Rankine-Gordon curve (the latter constitutes a safe under estimation of buckling strength) and intercept the multiple curve of resistance "*a*" of EC3 (2005). Again it is noteworthy to mention that RG curve is a semi-empirical formula that aims to determine the load capacity of columns from the plastic to the elastic slenderness range.

The RG column capacity associated with RG formula (and associated curve) is safe, since real columns although imperfect have higher resistant capacity (than the one's of RG) but with a specific margin of safety for each slenderness ratio.

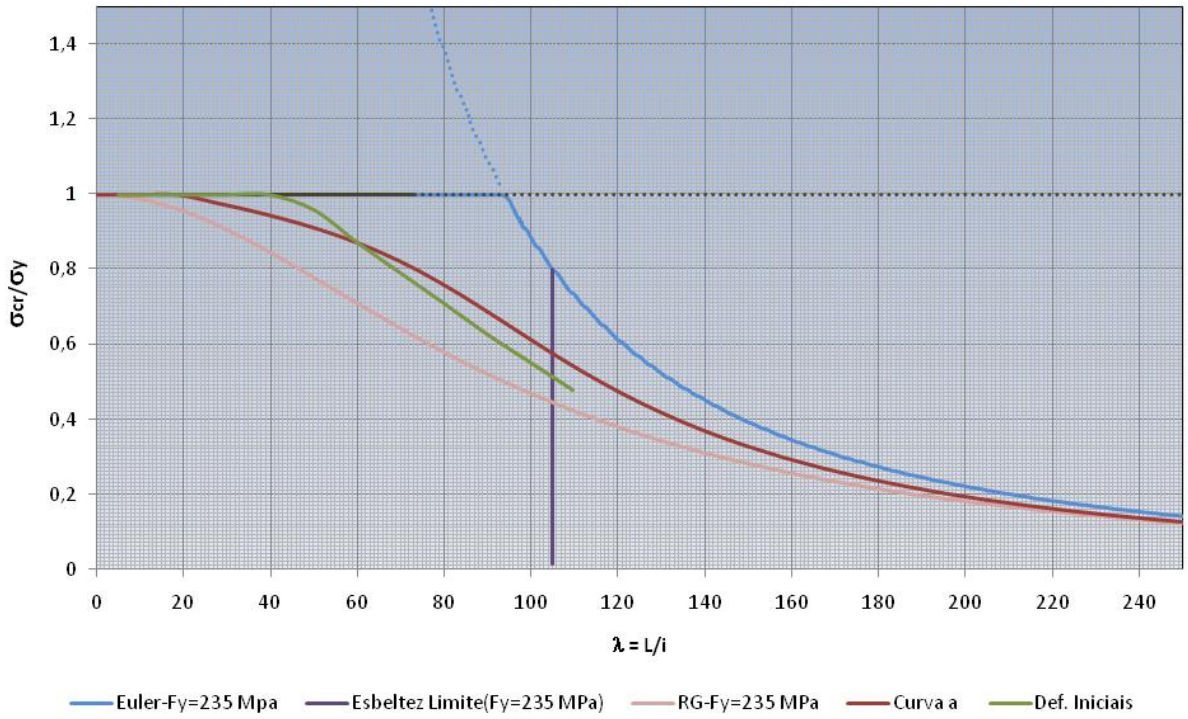

Figure 7: Theoretical design curves and Real Ultimate Capacity Curve
(for EC3 pattern of Initial Deformations)

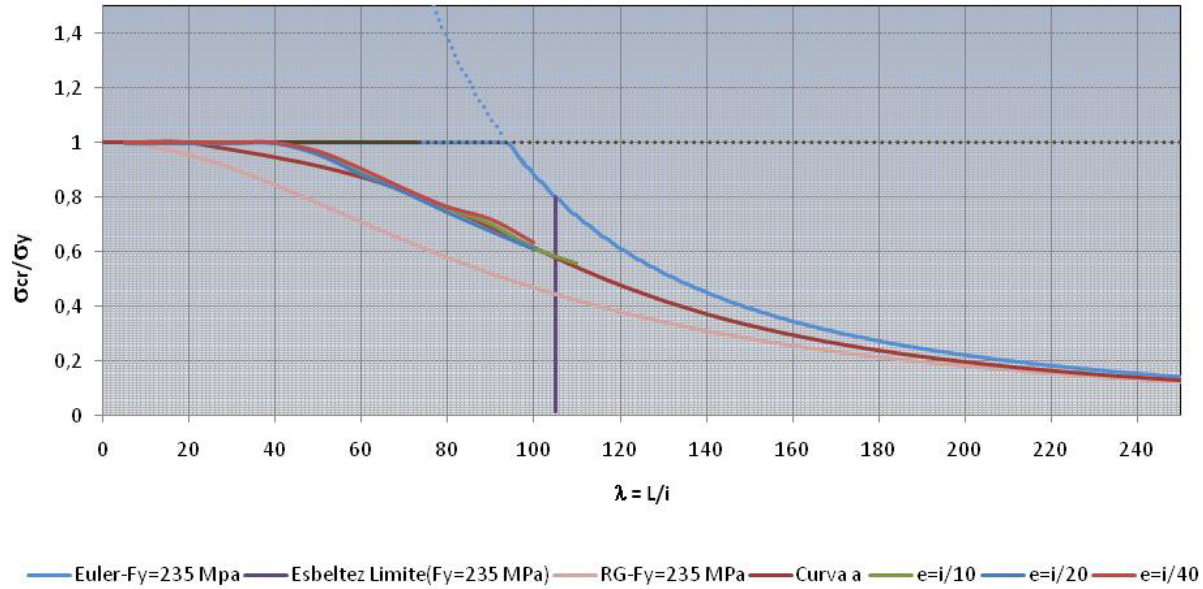

Figure 8: Theoretical design curves and Real Ultimate Capacity Curves for three eccentricity patterns

The buckling curves recommended in EC3, dependent on the geometrical characteristics of the columns, are intended to introduce in the design of structural elements the buckling effects that reduce the structural stability. This effect is introduced through the calculation of the buckling coefficient, which is multiplied by the yielding axial force by plastification to get the real axial bukling force taking into account geometric imperfections, residual stresses, among others.

From Figure 7 the Real Ultimate Capacity Curve for initial deformation, for slenderness below approximately 60, is above the buckling curve "*a*"; and for slenderness above approximately 60, such capacity curve is below the buckling curve "*a*". For slenderness below approximately 60, column capacity is controlled by elastic-plastic behavior as slenderness decreases, until a lower slenderness limit for which the column section crashes plastically for loads close to the squash load; reversely, for slenderness above approximately 60, column capacity tends to be controlled by elastic behavior (elastic instability) as slenderness increases.

Examining Figure 8, the Real Ultimate Capacity Curves obtained computationally – using Barros (1983) TBCOL software – for the three considered eccentricities, are above multiple resistance curve "*a*" (and therefore also providing bigger capacity than RG curve) for slenderness ratios in the approximate interval [40 , 80]; above slenderness value 80, curve "*a*" tends to be an asymptote of the column behavior for the eccentricity imperfection. In the dimensionless form represented little variability is in fact graphically seen; but for the same slenderness the ratio, the ratio critical stress versus yield stress decreases with increasing eccentricity. As expected it is verified, in ultimate stress terms, that increasing the eccentricity of the applied load leads to lower critical loads and therefore to smaller critical stresses.

SOME EXPERIMENTAL RESULTS OF THE AXIAL CAPACITY OF IMPERFECT CONCRETE-FILLED STEEL CIRCULAR TUBES

In this section are outlined the experimental results obtained for six columns of a set of 18 experimentally tested. They are composite steel-concrete columns (concrete filled steel tubes) in three groups of six columns each, of lengths respectively: 1.6, 1.7 and 1.8 meters. Each group of six steel columns of same length was filled with three types of concrete: 2 columns with current concrete C25/30; 2 columns with high strength concrete C45/55; and finally 2 columns with an improved high strength concrete C45/55, but with a smaller size of the inert providing for a better filling of spaces and potentially a better confinement.

Geometrically these 18 steel columns (of grade S235) – to be filled afterwards with the concrete grade mentioned earlier above – have an outside diameter of 90 mm and a thickness of 2 mm, but all have specific different patterns of initial deformations that were measured longitudinally along two perpendicular planes (XX and YY). These deformations are the result of fabrication transporting and handling of the columns, and are the so-called out-of-straightness initial deformations.

The experimental tests were carried out at LABEST universal compression testing machine at FEUP, with an actuator with 1000 kN maximum capacity, operating under a deformation control mode. The actuator was installed at the upper reaction beam of the testing steel frame; it incorporates a large rotation capacity loading plate, so that the upper end materializes a hinge support. To model bi-articulated column testing, a new hinge support for the lower end was fabricated made up of a semi-sphere – fixed on a bottom plate – on which rests a small collar that receives the bottom column end.

Two LVDT's were installed at the mid-height section of each column, along the above mentioned XX and YY orthogonal planes (Figure 9), with which the lateral deflections at mod-height were recorded at each step of the loading.

Although all the care was taken to minimize end eccentricities, these are un-avoidable in he upper end. In every column tested, after application of a 6 kN pre-load, the upper end eccentricities along XX and YY were carefully ascertained with mixed techniques using level, rotation meter and ruler; maximum accuracy of 1 mm is sufficient.

All columns were taken to ultimate capacity and beyond, looking for possible characterization of the post-buckling behavior until a sustained load approximately equal to 80% of the ultimate carrying capacity. Figure 10 shows one of such sustained cases, for column length of 1.80 meter. After testing the diameters (along x and along y axes) were measured at the mid-height cross section, in order to ascertain de degree of ovalization achieved.

Figure 9: Column test before

Figure 10: Column after testing

Table 1 synthesizes reference denominations of the six columns 1.8 meter long, as well as the corresponding concrete fill. Tables 2 and 3 synthesize capacity results, deformations and secant stiffness, respectively at ultimate point and at the sustained load of approximately 80% of the ultimate load.

Table 1 – References and properties of the 1.80 meter long concrete filled steel columns

Ref.	Altura	Diâmetro	Espessura	Aço	Betão		
	mm	mm	mm		C25/30	C45/55	C45/55-Melhorado
C.1.A.1	1800	90	2	X			X
C.1.A.2	1800	90	2	X			X
C.1.AB.45/55.1	1800	90	2	X		X	
C.1.AB.45/55.2	1800	90	2	X		X	
C.1.AB.25/30.1	1800	90	2	X	X		
C.1.AB.25/30.2	1800	90	2	X	X		

Figures 11-16 show simultaneously three types of column carrying capacity in graphical form, for the initial deflections pattern (out-of-straightness) specific of the columns, obtained by non linear geometric analysis using MIDAS/CIVIL software (2005): the capacity of the steel columns and the capacity of the composite steel-concrete columns (both for the initial imperfections characteristic of each column); and the capacity of the real columns tested under the corresponding initial imperfections but also of the unavoidable top end ecentricities.

Table 2 – Column ultimate load and corresponding deflection at mid-height of the 1.80 meter long concrete filled steel columns

Reference	Ultimate Load -- NLGA (steel tube)	Ultimate Load -- NLGA (steel tube filled with concrete)	Ultimate Load -- Exp. Tests (steel tube filled with concrete)	δ at Ultimate Load NLGA (steel tube)	δ at Ultimate Load NLGA (steel tube filled with concrete)	at Ultimate Load -- Exp. Tests (steel tube filled with concrete)
	(KN)	(KN)	(KN)	(mm)	(mm)	(mm)
C.1.AB.45/55.M1	330	685	436,52	4,25E-02	5,31E-02	1,65E-02
C.1.AB.45/55.M2	330	685	345,61	3,80E-02	4,77E-02	1,24E-02
C.1.AB.45/55.1	330	685	259,05	3,60E-02	4,48E-02	8,59E-03
C.1.AB.45/55.2	330	680	250,52	5,96E-02	5,86E-02	8,81E-03
C.1.AB.25/30.1	333	680	209,21	3,88E-02	4,71E-02	1,44E-02
C.1.AB.25/30.2	333	665	305,62	3,88E-02	5,71E-02	8,96E-03

Table 3 – Secant stiffness and corresponding deflection at mid-heigh for 80% ultimate load of the 1.80 meter long concrete filled steel columns

Reference	δsteel - 80% Ultimate Load	Ultimate Load - NLGA (steel) - δ (80% at ultimate load of steel tube)	Ultimate Load - NLGA (steel tube filled with concrete) - δ(80% at ultimate load of steel tube)	Ultimate Load -- Exp. Tests (steel tube filled with concrete) - δ(80% at ultimate load of steel tube)	Stiffness Limit - NLGA (Steel Tube)	Stiffness Limit - NLGA (steel tube filled with concrete)	Stiffness Limit - Exp. Tests (steel tube filled with concrete)
	(mm)	(KN)	(KN)	(KN)			
C.1.AB.45/55.M1	4,88E-03	264	544	368	5,41E+04	1,11E+05	7,54E+04
C.1.AB.45/55.M2	4,23E-03	264	544	256,91	6,24E+04	1,29E+05	6,07E+04
C.1.AB.45/55.1	4,16E-03	264	543,79	250	6,34E+04	1,31E+05	6,00E+04
C.1.AB.45/55.2	6,90E-03	264	544	247,36	3,83E+04	7,89E+04	3,59E+04
C.1.AB.25/30.1	3,31E-03	266,4	525,2	137,25	8,06E+04	1,59E+05	4,15E+04
C.1.AB.25/30.2	3,31E-03	266,4	458,86	266,73	8,06E+04	1,39E+05	8,07E+04

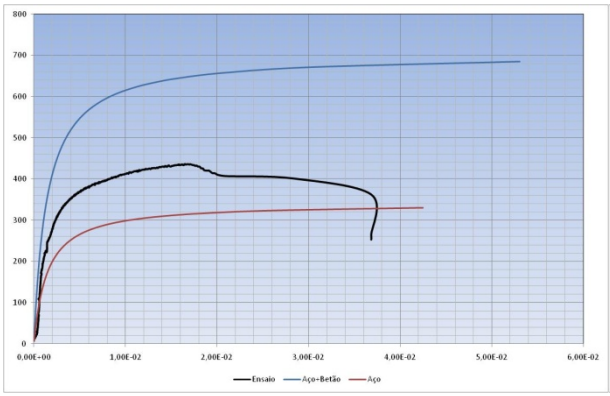

Fig.11 – Curves relating to column C.1.AB.45/55.M1

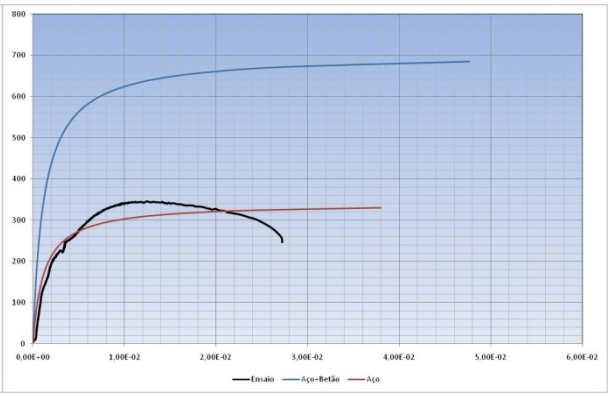

Fig.12 – Curves relating to column C.1. AB.45/55.M2

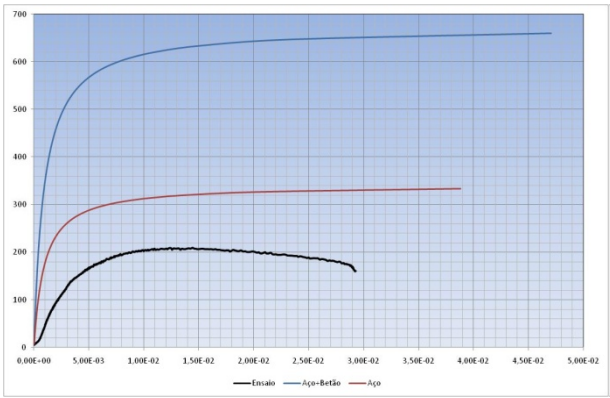

Fig. 13 – Curves relating to the column C.1.AB.25/30.1

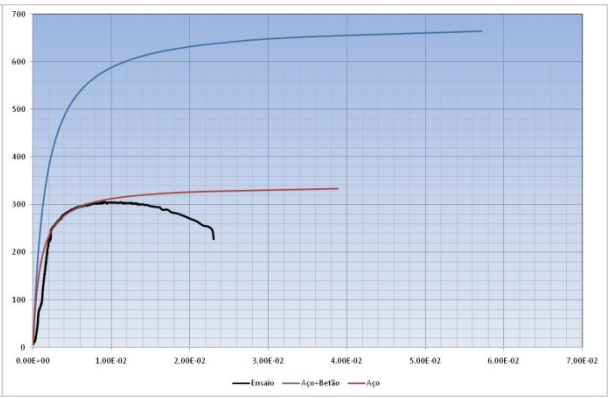

Fig.14 – Curves relating to the column C.1.AB.25/30.2

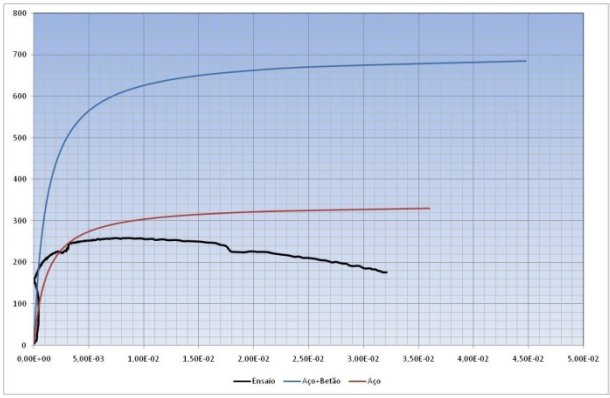

Fig.15 – Curves relating to the column C.1.AB.45/55.1

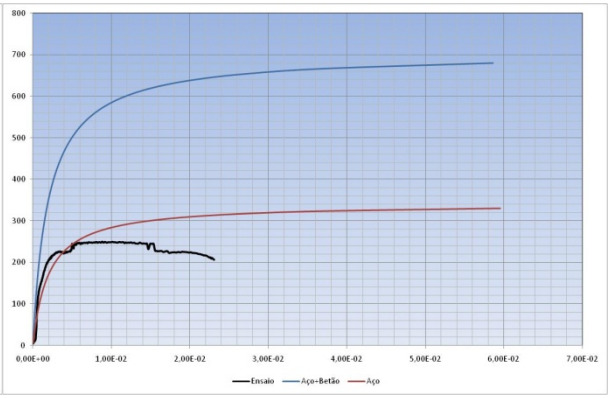

Fig.16 – Curves relating to the column C.1.AB.45/55.2

To understand the need to ascertain (with some accuracy) the top end eccentricities and their effect on the carrying capacity of composite concrete filled steel tubes, the composite column of Figure 11 was modeled with top end eccentricities of 0-5-7-8-10-15 mm along X-axis. In fact this specific column buckled in the XX plane, and the top end eccentricity was measured as a value approximately equal to 6 or 7 mm.

Figure 17 shows six nonlinear elastic trajectories on the loading plane of *Axial force versus Lateral displacement at mid-height* of the initially imperfect columns, corresponding to those six eccentricities mentioned above, for the composite steel-concrete column now with two simultaneous imperfections (deflections and eccentricities). The same comparison could be shown for the other columns of the 18 columns experimental testing program, with success both on the predicted behavior and on the eccentricities measured.

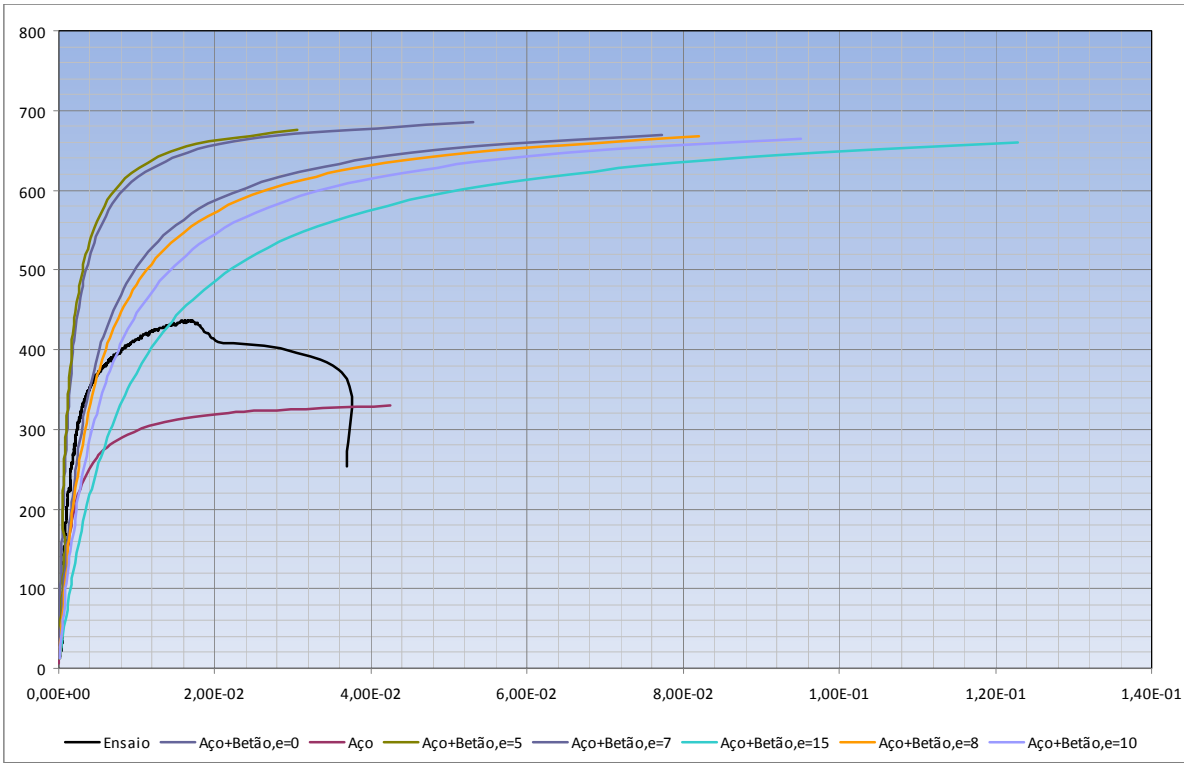

Figure 17: Nonlinear elastic trajectories of imperfect columns: steel column (without eccentricity) and composite steel-concrete column (with various top eccentricities) compared with the real column behavior

Analyzing the results presented some conclusions and observations can be taken.. As expected, the geometric nonlinear analysis shows that the composite columns have higher capacity and better performance than those solely in steel. This behavior is even more evident for higher resistance of the concrete core.

The curve of actual real column behavior is considerably apart from the composite steel-concrete column curve solely with initial deflections, which means that the top end eccentricities play an important role in predicting real column behavior.

Another potential source of justification for the discrepancy in results lies in the effect of confinement, which seems not to produce the expected effect. In fact the small cross section (that did not allow the vibratory probe to be introduced, mixing and conferring homogeneous characteristics to the concrete poured in the column) and the considerable size of the inert, are factors that when combined made it difficult to correctly concrete the columns; therefore each column is having significant presence of yet unseen voids (that a future cross-sectioning may reveal). This elation is supported by the fact that the columns with concrete belonging to the strength class C45/55 (but improved, because of smaller size inert) have better behavior and capacity than those of concrete with same class of resistance but with greater size of the constitutive inert.

The average gain in capacity by using composite columns, with a high strength concrete core, was 107% as compared to the capacity of solely steel columns. Those columns with normal strength concrete core, lead to average gains of 100% compared to steel columns (if confinement would be fully developed, higher gains or differences would be expected).

The secant limit stiffness of composite columns with concrete C45/55, has an average gain of approximately 106% compared to the secant limit stiffness of the steel columns. In turn, for columns of normal strength concrete core C25/30, that average gain was 85%.

Finally, for the same axial load, the composite columns allow for higher deformations than those solely in steel; for same lateral displacements, composite columns have obvious higher capacities. Confronting the results from tests with those resulting the non-linear geometric analysis, it appears that for equal axial load the steel column is more flexible and thus also reaches the buckling limit first. Further detailed results are listed in Tables 2 and 3.

SIMPLIFIED NONLINEAR MATERIAL ANALYSIS

The next step in this study will be the development of a simplified nonlinear material model, also using MIDAS/CIVIL (2005) software, to reproduce the real structural behavior. It is intended to use widespread commercial software as an alternative to some complex structural packages. However, the usual structural software are based on simple finite element formulation for structural elements such as beams and trusses that does not have the ability to manage nonlinear material behavior. In this case it is common to define a local nonlinear material behavior. The software employed in this work makes use of two different procedures to define this local nonlinear material behavior, namely: Plastic hinge model (PHM) and Fiber model (FM). The main difference between the two models lies in the way the constitutive laws are defined and used.

The fiber model (FM) was selected as a potential simplified nonlinear material model since is based on the discretization of a section in elements or fibers that are associated to each material with axial deformation only (Figure 18). Thus, in this methodology a global curve is not defined for a section (the envelope curve), but with the constitutive laws of the materials that compose the section. The envelope law is then determined through an increasing variation of the rotation/moment relation. The software using the fiber model is based on the following limitations: the section shape remains unchanged in the deformation process (though remains perpendicular to neutral axis) and, therefore, slipping is not considered.

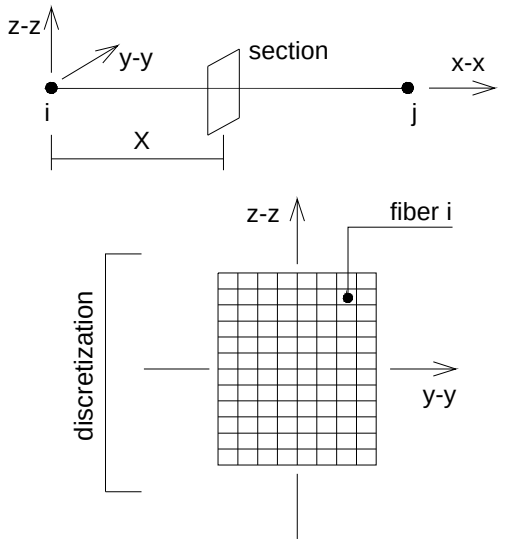

Figure 18: Fiber model and section discretization.

In the FM the state of each fiber is evaluated through the corresponding axial deformations due to axial force and also fiber flexion deformations. The axial force and the flexion moment of the section are then calculated from the tension level in each fiber. The section properties insuring nonlinear behavior are defined through a tension-extension relation (stress-strain) of the fibers that constitutes the all section.

The materials constitutive laws have to rigorously reproduce the real behavior in order to get a reasonable section envelope of the member and structure that is intended to study. The experimental steel tensile test allows characterizing with sufficient rigorousness its mechanical behavior. However the concrete uniaxial compression test does not allow characterizing this material conveniently due to lateral confinement that significantly increases the resistant capacity. In this in case an adjustment process must be carry out to set the parameters that reproduce the experimental behavior. The characteristics of the materials that will be used are in accordance with those that were used in the experimental procedure, except for the concrete confinement for which successive attempts were made to obtain plausible confinement value.

Additionally, this model has the advantage of tracing the section moment-rotation relationship, the monitoring of the neutral axis position and the possibility to establish the axial force level in each fiber. If some sections are used, it is also possible to determine the extension of the plastic hinge zone which could also be one of the outcomes of this study.

ON THE USE OF THE INTERACTIVE EQUATION FOR CIRCULAR TUBULAR STEEL SECTION COLUMNS

It is well known that mild steel is the almost perfect material for plastic analysis and design, namely in structural civil engineering domain. In that context one form of modern constructions is based on the use of steel framed structures with joints capable of transmitting bending moments, either rigid or semi-rigid joint framed structures.

In such steel structures, designed through considerations of plastic analysis and plastic design, the applied forces are resisted mainly by bending moments and shear forces in the structural members; therefore member sections must carry simultaneously a combination of direct normal stresses σ (due to bending moments) and shear stresses τ (due to shear forces), for which Tresca or Von Mises yield criteria [Popov, 1968] [Silva, 1995] [Branco, 1998] are the most common to determine the start of yield when

$$\left(\frac{\sigma}{\sigma_y}\right)^2+\left(\frac{\tau}{\tau_y}\right)^2=1 \begin{cases} \textit{Tresca} & \begin{cases} \sigma_1>\sigma_2 \;\; \textit{and both same sign} \\ \qquad \sigma_1=\underline{\sigma_y=2\tau_y} \end{cases} \Rightarrow \underline{\underline{\sigma^2+4\tau^2=\sigma_y{}^2}} \\ \begin{cases} \sigma_1>\sigma_2 \;\; \textit{but of opposite sign} \\ \qquad \sigma_1-\sigma_2=\underline{\sigma_y=2\tau_y} \end{cases} \\ \textit{Von Mises} \quad \sigma_1{}^2+\sigma_2{}^2-\sigma_1\sigma_2=\underline{\sigma_y{}^2=3\tau_y{}^2} \Rightarrow \underline{\underline{\sigma^2+3\tau^2=\sigma_y{}^2}} \end{cases} \tag{1}$$

where (σ_1,σ_2) are sectional direct principal stresses, and (σ_y,τ_y) are respectively the yield stresses in pure bending and pure shear for each member section.

The existing axial forces will normally have a secondary importance, except in the columns. In steel framed structures, especially those of heavy industrial construction or of tall steel buildings, columns may have to carry quite significant axial forces in addition to bending moments. The effect of axial force in members is to move the neutral axis in relation to its position when axial force is non-existent or negligible.

For structures analyzed and design under plastic design philosophy, the axial force is the major factor that can alter the plastic moment (besides the obvious cross-section dimensions and sectional shape); it is well known that the alterations of sectional plastic moment due to shear forces are much smaller than those created by axial forces, and need only to be considered in rare cases when shear forces are quite large. So in high-rise structures the axial force effects on plastic moment reduction are important, although in those cases also instability is more likely to be the controlling factor.

By changing the position of the sectional neutral axis, the increase of the axial force P reduces the plastic moment bending capacity of the section $M_{p,reduced}$. This effect is analytically translated by the bending moment-axial force interaction equation.

Traditionally deduced and easily explained for full rectangular cross sections ($b \times h$), for which the bending moment-axial force interaction equation is

$$\frac{M_{p,reduced}}{M_p} = 1 - \left(\frac{P}{P_p} \right)^2 \tag{2}$$

it can also be easily extended for I-sections (with two possible locations of the neutral axis in the web or in the flange) [Massonnet y Save, 1966]. The plastic moment of the full rectangular section under pure bending is $M_p = \sigma_y \frac{bh^2}{4}$, while the maximum axial force that the section can carry before crushing occurs with yield of all the section fibers under the so-called squash load (or plastic crushing load) is $P_p = \sigma_y \, bh$.

Since for full rectangular sections the reduction term is $\left(\frac{P}{P_p} \right)^2$, both tensile and compressive axial forces reduce equally the plastic moment of those sections as shown in non-dimensional form by the interaction curve represented in Figure 19; the latter figure also represents the interaction curve for the I-section (457 × 152 UB 82) as adapted from Moy (1981).

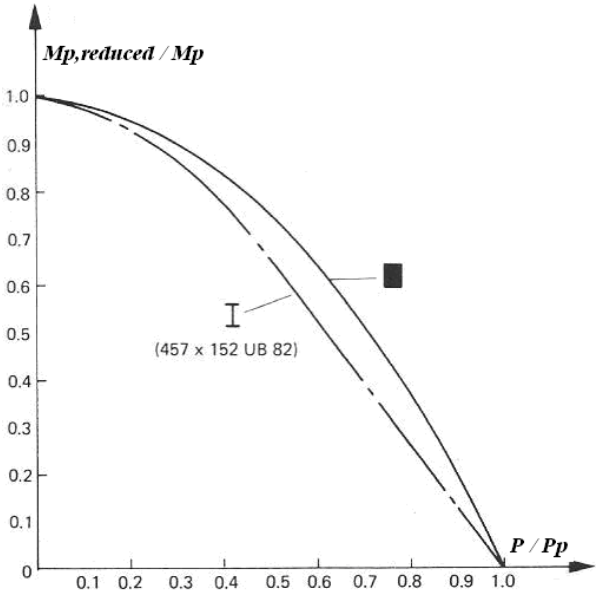

Figure 19: Interaction curve for full rectangular section and for an I-section

Barros (2004) applied the latter interaction equation for characterising approximately the elasto-plastic carrying capacity of experimental circular tubular section column (# 3) [Barros, 1983], assuming (approximately but irregularly) the interaction equations to be the same for both sections. Then such approximate interaction equation was found as $\frac{P(\alpha+w)}{172.29}+\left(\frac{P}{40496}\right)^2=1$ from which $172.29\,P^2+40496^2(\alpha+w)P-172.29\times40496^2=0$, where α measures the initial imperfection (initial eccentricity or deformation) at mid-height and w is the lateral mid-height deflection under axial force *P*. The *Curve of Plastic Unloading* of the beam-column – translating the equilibrium in the deformed configuration corresponding to the formation of the plastic collapse mechanism with a plastic hinge at mid-height – is obtained solving previous equation for *P* in the form:

$$P(w)\cong -4.759\times10^6\times(\alpha+w)+\sqrt{22.65\times10^{12}\times(\alpha+w)^2+40496^2} \tag{3}$$

For $w=0$, the previous expression determines the plastic limit load P_p (squash load or plastic crushing load) that represents the limit axial load for a 1st order plastic analysis.

Herein the interaction equation for circular tubular section is presented as deduced by Barros (2009). Consider that Figure 20 below represents a circular tubular cross section, with outside diameter D and thickness t, under flexion-compression; although the compressive force P is such that neutral axis position is altered from its central position of pure bending, the resulting stress distribution can be replaced by the sum of two distinct stress distributions: one central distribution with stress resultant P and the other a peripheral distribution (of two symmetric portions) with stress resultant M. As the bending moment increases, curvature also increases; yielding spreads toward the neutral axis, with stress limited to the yield stress σ_y but strain increasing enormously because of plastic flow.

The angle $\varphi/2$ is measured from the vertical axis and locates (symmetrically) the depth of the circular tubular section that has already yielded in flexion; it corresponds to a reduced plastic moment $M_{p,reduced}$ (under sustained compression P). The central core beyhond $\varphi/2$ ($0<\varphi/2<\pi/2$) corresponds to the remaining capacity to yield under P.

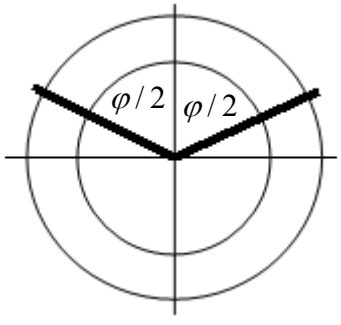

Figure 20: Circular tubular cross section

As was deduced by Barros (2009) -- and for sure elsewhere as used for instance in a somehow similar form in ASCE (1978) including nonlinear geometric effects by a moment amplification factor -- the interaction equation of circular tubular cross sections is expressed by:

$$\begin{cases} \dfrac{P}{P_p} = \dfrac{\pi-\varphi}{\pi} = 1-\dfrac{\varphi/2}{\pi/2} \Rightarrow \dfrac{\varphi}{2} = \dfrac{\pi}{2}\left(1-\dfrac{P}{P_p}\right) = \dfrac{\pi}{2} - \dfrac{\pi}{2}\dfrac{P}{P_p} \\ \dfrac{M_{p,reduced}}{M_p} = \sin\left(\dfrac{\varphi}{2}\right) = \cos\left(\dfrac{\pi}{2}\dfrac{P}{P_p}\right) \end{cases} \tag{4}$$

in which the plastic moment in pure bending M_p and the squash load (or plastic crushing load) P_p of circular tubular cross sections [Massonnet y Save, 1966] are respectively:

$$M_p = \sigma_y \frac{D^3}{6}\left[1-\left(1-\frac{2t}{D}\right)^3\right] \tag{5}$$

$$P_p = \sigma_y \frac{\pi D^2}{4}\left[1-\left(1-\frac{2t}{D}\right)^2\right] \tag{6}$$

The reduced plastic moment $M_{p,reduced}$, allowing for the axial force P, resists the rotation. Also, for any pattern of column lateral displacements, the reduced plastic moment $M_{p,reduced}$ of the collapse axial load P_c causes the column rotation at collapse.

Then the exact interaction equation was found as $\dfrac{M_{p,reduced}}{M_p} = \cos\left(\dfrac{\pi}{2}\dfrac{P}{P_p}\right) = \cos\theta \approx 1-\dfrac{\theta^2}{2}$ from which $\dfrac{P(\alpha+w)}{111.84} + 1.2337\left(\dfrac{P}{33206.8}\right)^2 \approx 1$ so that the more exact *Curve of Plastic Unloading* of the circular tubular section beam-column is now expressed by:

$$P(w) \cong -3.9959\times10^6 \times(\alpha+w) + \sqrt{15.9676\times10^{12}\times(\alpha+w)^2 + 29896.63^2} \tag{7}$$

The previous considerations are valid for sections of structural members that are not affected by instability or buckling considerations. In such cases, the effects of axial force and lateral deflection are quite disturbing. Very stiff structures collapse at the plastic collapse load P_p, while very flexible structures buckle at the elastic critical load P_{cr}. Merchant developed a numerical formula to approximate the true collapse load (factor), based on the Rankine amplification factor used in strut analysis. So, using the so-called formula of Merchant-Rankine (FMR)

$$\frac{1}{P_{cr}} + \frac{1}{P_p} = \frac{1}{P_u} \tag{8}$$

leads to more accurate estimates of the ultimate load P_u or collapse column load [Moy, 1981]. When compared with experimental results of several tested frames, the estimates obtained by FMR revealed to be safe approximations of the observed and theoretical collapse load factors (close to but lower than).

For the column # 3 used earlier by Barros (1983, 2004) with the following known column data -- $(P_u)_{exact} = 6266\,N$, $(P_u)_{\exp} = 6470\,N$, $P_{cr} = 8354\,N$ -- the irregular approximation (using the rectangular section interaction equation) in conjunction with the FMR, led to (the not so precise or valid) Table 4 of results:

Table 4 - Estimates of the ultimate load P_u by an irregular approximation [Barros, 2003]

α	P_p	$(P_u)_{\substack{approx \\ FMR}}$	Δ_{exact}	Δ_{exp}
(mm)	*(N)*	*(N)*	*(%)*	*(%)*
1.16	35350	6757	7.8	4.4
2	32081	6628	5.8	2.4
3.16	***28160***	***6443***	***2.8***	***-0.4***

Figure 21 condensates the determination of the ultimate load P_u by FMR, in the context of the initial defect or initial imperfection "initial eccentricity *and* initial deformation".

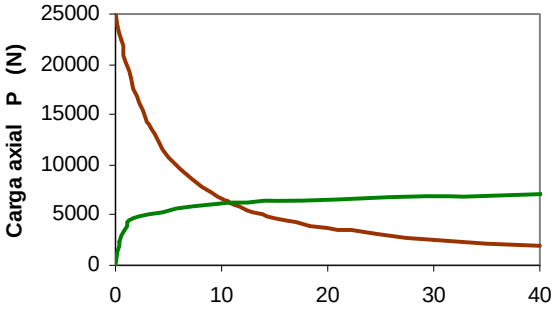

Figure 21: Determination of the ultimate load P_u by FMR, with $(\alpha \approx 3.16\,mm)$

Using now the exact interaction equation of circular tubular section (for the same column # 3) in conjunction with the FMR, the following more valid table of results was obtained:

Table 5 - Estimates of the ultimate load P_u using the exact interaction equation [Barros, 2009]

α	$\boldsymbol{P_p}$ $(w=0)$	$(P_u)_{\substack{approx \\ FMR}}$	Δ_{exact}	Δ_{exp}
(mm)	*(N)*	*(N)*	*(%)*	*(%)*
0	29897	6529	4.1	0.9
1.16	***25619***	***6299***	***0.5***	***-2.6***
2	22955	6125	-2.2	-5.3
3.16	19827	5878	-6.2	-9.1

For steel applications Wood (1974) suggested the use of a modified version of the FMR (herein labelled FMR modified), as mentioned by Moy (1981) Reis e Camotim (2001) and others, expressed in terms of loads (or equivalently in terms of load factors λ) in the form:

$$\begin{cases} P_u = P_p & \text{for} \quad \dfrac{P_{cr}}{P_p} > 10 \\ \dfrac{1}{P_u} = \dfrac{1}{P_{cr}} + \dfrac{\kappa}{P_p} & \text{for} \quad 10 > \dfrac{P_{cr}}{P_p} > 4 \quad \text{and} \quad \kappa = 0.9 \end{cases} \tag{9}$$

This modification agrees more closely with the experimental results than the classic FMR as can be seen, in Figure 22 adapted from Moy (1981), by the two straight lines in the Merchant-Rankine interaction diagram: full line is FMR, dashed line is FMR-modified.

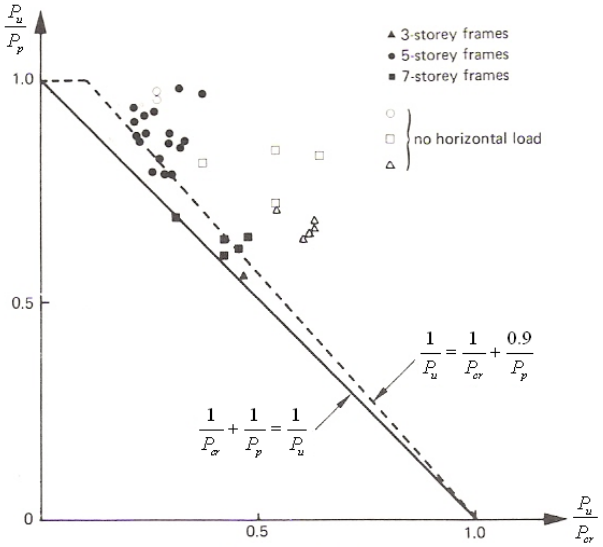

Figure 22: Merchant-Rankine interaction diagram: FMR and FMR-modified

Using now the exact interaction equation of circular tubular section (for the same column # 3) in conjunction with the FMR-modified, the more accurate (and also valid) table of results for the ultimate column load P_u is now corrected to values of the order of magnitude of the one's obtained earlier with an irregular approximation (Table 4).

Table 6 - Estimates of ultimate load P_u using the exact interaction equation with the FMR-modified [Barros, 2009]

α	P_p ($w=0$)	$(P_u)_{FMR\ \text{modified}}$
(mm)	*(N)*	*(N)*
0	29897	6675
1.16	***25619***	***6459***
2	***22955***	***6293***
3.16	19827	6057

The adequate use of the FMR and of FMR-modified, in the context of tubular steel columns, reveals promising. Because of that, it is expected that the complete experimental program of the 18 composite columns might lead to a practical determination of κ in equation (9) that would be applicable to composite columns.

CONCLUSIONS

Tubular members (hollowed or concrete-filled) and tubular structures have nowadays a quite justifiable widespread use in Civil Engineering. The comparison between theoretical predictions (using TBCOL program) and design curve predictions of the critical stresses, for a wide range of slenderness ratio, was valid and useful. For columns made of steel S235 with initial deformations and slenderness below about 60, columns capacity is controlled by elastic-plastic resistant and performance, as the slenderness decreases (until the minimum limit, controlled by crushing or plastic squash).

For columns with slenderness above 60, columns capacity tends to be controlled by elastic instability as slenderness increases. For steel S235, in the dimensionless plot of critical stress divided by steel yield stress versus slenderness, the parametric effect of the end-eccentricities is only slightly significant for slenderness between 40 to 80. The Rankine-Gordon formula leads to a design curve that always gives conservative safe estimates of the resistant column capacity, for distinct column imperfections; such safety factor depends on slenderness.

The results of the tests of composite columns reveal some of the strength advantage of using composite construction over traditional steel constructions. They also show the importance of top end eccentricities in the results, and the needed care to ascertain their value (with accuracy of about 1-2 mm) in view of needed adjusted results of computational or numeric versus theoretical analyses. Some capacity gains are outlined, as well as some ductility reductions given in tabular form; reasons for possible discrepancy of results were mentioned, in view of the small scale of column sections. The interaction equation for circular section tubes was introduced, and the use of Merchant-Rankine formula (FMR) was justified through an example. A modified version of FMR was also applied in the pure context of steel tubes, but its potential extension for composite concrete-filled tubes was suggested.

ACKNOWLEDGEMENTS

The experimental part of this work was done at FEUP laboratory LABEST of the Civil Engineering Department. The authors acknowledge LABEST Director, Prof. J.A. Figueiras, for allowing this first testing sequence of 18 composite columns to characterize and assess the strength capacities of concrete-filled steel tubes. Special thanks are also due to the operator of the universal testing machine, Engª Paula Silva, for her availability and professional interest is achieving these results.

REFERENCES

ASCE, *Inelastic Behavior of Members and Structures*, ASCE Annual Convention & Exposition, Combined Preprint for Session 45, Paper by D.R. Sherman "Cyclic Inelastic Behavior of Beam-Columns and Struts", pp. 23-54, Committee on Tubular Structures, Chicago, Illinois, October 16-20, 1978.

R.C. Barros, *Buckling Analysis of End Restrained Imperfect Tubular Beam Columns*, Ph.D. Dissertation, The University of Akron, Akron, Ohio, U.S.A., March 1983.

R.C. Barros, "Sobre a Extrapolação de Resultados Experimentais em Problemas Estruturais de Instabilidade e Vibrações", Revista *Mecânica Experimental*, Edição da Associação Portuguesa de Análise Experimental de Tensões (APAET), Nº 10, pp. 1-12, LNEC, Lisboa, Portugal, 2004.

R.C. Barros, "On the Determination of the Interaction Equation of Circular Tubular Sections of Steel Tubular Columns", Deptº Engª Civil, Secção de Estruturas, F.E.U.P., 14th February 2009.

C.M. Branco, *Mecânica dos Materiais*, 3ª edição, Fundação Calouste Gulbenkian, Lisboa, Novembro 1998.

EC 3 - European Committee for Standardization, *Eurocode 3: Design of steel structures - Part 1-1 General rules and rules for buildings*. 2005, CEN: Brussels.

C. Massonnet y M. Save, *Calculo Plastico de las Construcciones*, Tomo I: Estructuras Planas, Montaner y Simon S.A., Barcelona, 1966.

MIDASIT - MIDAS/CIVIL, "General purpose analysis and optimal design system for civil structures", MIDAS Information Technology Co, Ltd., Korea, 2005.
S.S.J. Moy, *Plastic Methods for Steel and Concrete Structures*, A Halsted Press Book, John Wiley & Sons, New York, 1981.
E.P. Popov, *Introduction to Mechanics of Solids*, Prentice-Hall Inc., Englewood Cliffs, N.J., U.S.A., 1968.
A. Reis e D. Camotim, *Estabilidade Estrutural*, Editora McGraw-Hill de Portugal Lda, Amadora, Portugal, 2001.
V.D. Silva, *Mecânica e Resistência dos Materiais*, Ediliber Editora, Coimbra, 1995.
R.H. Wood, *Effective Lengths of Columns in Multistorey Buildings*, BRE Current Paper 85/74, U.K., September 1974.

BIBLIOGRAPHY

Allen H. G., Bulson P. S., *Background to Buckling*, McGraw-Hill Book Company Limited, U.K., 1980.
Arguelles Alvarez, R.; Arguelles Bustillo, R.; Arriaga Martitegui, F.; Reales Atienza, J.R.; *Estructuras de Acero,* Volume 1, M.B.H. Bellisco, Ediciones Técnicas y Cientificas; 2ª Edição, Madrid, 2005.
Romero, M.L.; Bonet, J.L. and Ivorra, S.; "A review of nonlinear analysis models for concrete filled tubular columns", *Innovation in Civil and Structural Engineering Computing*, Saxe-Coburg Publications, 2005.